Polymer 51 (2010) 832–841

Contents lists available at ScienceDirect

Polymer

journal homepage: www.elsevier.com/locate/polymer

Hybrid organic–inorganic materials using zirconium based NBBs and vinyl trimethoxysilane: Effect of pre-hydrolysis of silane

R. Di Maggio [a,*], S. Dirè [a], E. Callone [a], F. Girardi [a], G. Kickelbick [b]

[a] Dept. Mat. Eng. Ind. Technol., University of Trento, Trento, Italy
[b] Institute of Materials Chemistry, Vienna University of Technology, Vienna, Austria

ARTICLE INFO

Article history:
Received 8 July 2009
Received in revised form
4 December 2009
Accepted 19 December 2009
Available online 4 January 2010

Keywords:
I/O hybrid
Zirconium oxocluster
Vinylacetic acid

ABSTRACT

Various Nano Building Blocks (NBBs) such as polyhedral silsesquioxanes (POSS), functionalized metal oxide particles and transition metal oxoclusters have been already developed and used to improve thermal and mechanical properties of organic polymers. The NBBs ideal for the preparation of hybrid materials and nanocomposites are monodispersed, well-defined objects capped with polymerisable functions suitable for copolymerisation with organic monomers.

In this study zirconium oxoclusters (ZrNBB) were obtained as a crystalline precipitate by reaction between zirconium propoxide and vinylacetic acid. They were post-functionalised by copolymerisation with vinyl trimethoxysilane in different molar ratios. The hybrid samples were prepared both with the organosilane pre-hydrolysis step and without adding water. Hybrid materials were obtained through the radical polymerization process by adding benzoyl peroxide (BPO). Silane pre-hydrolysis prevents bulk samples from being obtained.

The polymerization process was studied using differential scanning calorimetry (DSC), and the shear storage modulus (G') and loss modulus (G'') of hybrid polymers were investigated by dynamic mechanical spectroscopy (DMS). Multinuclear liquid- and solid-state NMR analyses and Fourier transform infrared (FTIR) spectroscopy were used to characterize the reagents and hybrid materials, and to study the influence of the synthesis conditions on condensation and polymerization.

1. Introduction

Hybrid inorganic–organic polymers based on ZrO_2–SiO_2 inorganic components have attracted much interest in the recent years, due to their potential applications in areas from catalysis to optics [1–7]. It is essential to control the material's final architecture via well-defined reaction steps from molecular level onwards in order to obtain materials with enhanced properties. This is particularly true for the preparation of multi-component oxide systems using the sol–gel process. The mismatch between the hydrolysis and condensation rates of the precursors represents a drawback of sol–gel synthesis, because the materials obtained can be heterogeneous [8]. Different approaches to synthesis have been developed to prevent phase separation in multi-component systems. Recent approaches used for the preparation of homogeneous inorganic–organic hybrid materials were based on mixing metal alkoxides with methacrylic acid and/or methacryloxysilane [2,9–11]. The high temperature treatment of these multi-component hybrid materials led to binary oxide phases, MO_2–SiO_2 with M = Zr, Ti, Hf [12].

Recently, the reaction of pre-hydrolyzed methacryloxypropyl trimethoxysilane (MPTMS) with transition metal oxoclusters $M_4O_2(OMc)_{12}$ (M = Zr, Hf) was studied with a view to producing mixed oxides after high temperature thermal treatment. The procedure was based on the organosilane hydrolysis-condensation step, followed by copolymerisation between the methacrylate groups linked to the siloxane network and those capping the metal oxoclusters [13–15].

So far, zirconium oxoclusters such as $Zr_6O_4(OH)_4(carboxylate)_{12}$ and $Zr_{12}O_8(OH)_8(carboxylate)_{24}$ have been used mainly in a free radical polymerization process as inorganic cross-linking agents for organic polymers [7–17]. Their influence on the material's final properties depends on the load of zirconium oxoclusters, on their functionalization and polymerization conditions [18–23]. It has also been demonstrated that the physical entrapment of Zr12 clusters, acting as inorganic nanofillers, was able to modify the thermal and mechanical properties of polystyrene [21,24].

With a view to producing inorganic–organic hybrid materials for high temperature applications, we recently reported our preliminary findings on the copolymerisation of vinyl-acetate-

* Corresponding author. Tel.: +39 461 882419; fax: +39 461 281977.
E-mail address: rosa.dimaggio@unitn.it (R. Di Maggio).

0032-3861/$ – see front matter © 2009 Elsevier Ltd. All rights reserved.
doi:10.1016/j.polymer.2009.12.026

substituted zirconium oxoclusters and vinyl trimethoxysilane (VTMS) [25]. To prevent large oligosiloxane formation and improve the dispersion of the two inorganic compounds at molecular level, the organosilane was not reacted with water in a hydrolytic step before radical polymerization.

To obtain homogeneous polymer-nanocomposite materials, this study was aimed to explore how oxoclusters load and water could affect polymerization and polycondensation processes in hybrid materials prepared from VTMS and ZrNBB, using different ratio of the precursors. We studied the influence of synthesis conditions on the structure-related properties. The hybrid materials prepared in this work have a marked inorganic content and behave as thermosetting polymers. Particular attention has been devoted to the thermo-mechanical properties up to 300 °C of the best-suited hybrid silica–zirconia containing materials.

2. Experimental part

2.1. Materials

The reagents were purchased by Aldrich and used as received, without any further purification.

2.2. Synthesis

2.2.1. Zirconium oxoclusters synthesis

Zirconium *n*-propoxide and vinylacetic acid (VAA) were mixed in 1:4 molar ratio under N_2 atmosphere and the clear solution was left at room temperature until colorless crystals formed by precipitation (sample label: ZrNBB).

The ZrNBB elemental analysis (C, 36.74; H, 4.14; Zr, 25.20 wt%) suggests the following theoretical formula: $[Zr_6O_4(OH)_4(OOCCH_2CHCH_2)_{12}(n\text{-PrOH})]_2\cdot 4(CH_2CHCH_2COOH)$.

2.2.2. Synthesis of ZrNBB/VTMS hybrids without silane pre-hydrolysis

The ZrNBB crystals were dissolved in tetrahydrofurane (THF) (0.06 M) and vinyltrimethoxysilane (VTMS) was added to the solution while stirring in air at room temperature. Different solutions were prepared with the Zr:Si molar ratio ranging from 1:1 to 1:20. The amount of benzoyl peroxide (BPO) corresponding to 1 wt% of VTMS and ZrNBB was added to the mixture. After 24 h, the solution was concentrated to dryness under a reduced pressure and the obtained xerogels, labelled ZrNBB/VTMS, were thermally cured at 90 °C for 4 h and at 130 °C for 1.5 h. The evaporation of solvent, required to dissolve the oxocluster crystals, covers important thermal effects in DSC curves, making the analysis of polymerization process difficult.pg The solvent is thus evaporated before the thermal treatment.

For the sake of comparison, two samples, labelled ZrNBB/BPO and VTMS/BPO, were prepared by dissolving the pure reagents, ZrNBB and VTMS, 0.06 and 0.6 M respectively, in THF and BPO (1%wt of the reagents).

2.2.3. Synthesis of ZrNBB/VTMS hybrids with silane pre-hydrolysis

The hybrid samples were also prepared with a pre-hydrolysis step. The silane was dissolved in THF (0.6 M) and then reacted with acidic water (HCl) with molar ratio of $Si:H_2O = 1:3$ [26]. ZrNBB was then added to the mixture and the synthesis of the hybrid xerogels was performed as described above.

2.3. Measurements

Solubility experiments were conducted by swelling the samples in deionized water, *n*-hexane and toluene at 25 °C. The samples were kept in a vacuum and weighed (W_0) before swelling in solvent. After 4 days, the solvent was removed and the swollen samples were allowed to dry. The final weight was measured (W_f) and the soluble fraction S was calculated from $S = 100(W_0 - W_f)/W_0$ [27].

Differential scanning calorimetry analyses were performed using a DSC92 SETARAM, in N_2 with a 10 °C/min heating rate.

Dynamic mechanical spectroscopy (DMS) was performed in shear mode on cured hybrid materials with a cylindrical shape with parallel planar surfaces 12 mm^2 in area and 3.5 mm thick, using a Seiko DMS 6100 instrument at a frequency of 1 Hz, with a 0.005 mm displacement in the direction of the diameter. The test was performed in air, applying 1000 mN as the starting force, heating at a rate of 2°C min^{-1} up to 300 °C. The shear storage modulus (G'), loss modulus (G'') and tan δ were measured. The T_g was measured by collecting the temperature of the maximum loss modulus curve.

FTIR spectra were recorded in transmission mode in the range of 4000–400 cm^{-1} on KBr pellets (64 scans and 2 cm^{-1} resolution), using a Thermo Optics Avatar 330 FTIR instrument.

Solid state NMR analyses were conducted with a Bruker 400 WB instrument, applying a carrier frequency of 400.13 MHz (^1H). The 1D experiments were based on single pulse sequence under the following conditions: ^{29}Si at 79.50 MHz with $\pi/2$ 4.3 μs at −2 dB and a 10 s delay time; ^{13}C at 100.07 MHz, $\pi/2$ 3.5 μs at −1.7 dB, 5.3 μs decoupling pulse and a 10 s delay time; 2D ^{13}C–^1H hector experiments with LG-RF 73529 Hz, 2.5 s delay time, 200 μ contact time s, decoupling and excitation pulse −4.2 μs. Samples were packed in 4 mm-zirconia rotors, which were spun at 9.5 kHz under an air flow.

Classical T^n and Q^n notations are used to represent three and four functional silicon units, respectively, with *n* being the number of oxobridges. Throughout the text, the carbon atoms and the related bonded protons are identified by numbers, according to Scheme 1 below.

3. Results

3.1. Structural characterization of zirconium oxoclusters

Several studies on carboxylate surface-functionalized zirconium oxoclusters by Schubert et al. [18] showed that this class of compounds can have various shapes, depending on the nature of carboxylic acid and the ratio of metal alkoxide to carboxylic acid [28,29].

As reported in the experimental part, the calculated molecular formula of ZrNBB from the elemental analysis is $[Zr_6O_4(OH)_4(OOCCH_2CHCH_2)_{12}(n\text{-PrOH})]_2\cdot 4(CH_2CHCH_2COOH)$. The crystalline structure of the vinyl-acetate-substituted Zr clusters (not reported

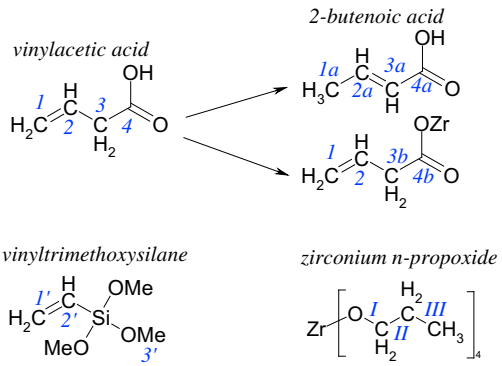

Scheme 1. Structural elucidation of reagents and derivates (the numbers refer to different carbon atoms and related protons).

here) was determined and found consistent with the structure of Zr12 clusters described by Schubert et al [18–21,30–32]. According to the previously published results [21], ZrNBB can be described as dimers of Zr6 clusters characterized by different arrangements of VAA ligands, which may be terminal, chelating and bridging. The two Zr6 clusters are linked by bridging carboxylate groups, and form the Zr12 cluster.

The ZrNBB crystals are colorless and do not dissolve in water, but are soluble in various organic solvents, such as toluene, THF and ethyl acetate. The structural characterization of ZrNBB was done using FTIR and NMR. The main features are summarized below and are consistent with data reported in elsewhere [18,25].

The FTIR spectrum of ZrNBB [25] shows the stretching vibrations of OH groups at 3400 (sharp, Zr–OH) and 3242 cm^{-1} (broad, VAA). The typical vibrations of vinyl acetate groups occur at 3072 cm^{-1} ($\nu_{as\ CH2,\ vi}$), 3022 cm^{-1} ($\nu_{s\ CH2,\ vi}$), 1706 cm^{-1} ($\nu_{C=O}$), 1644 and 1602 cm^{-1} ($\nu_{C=C}$), 1556 and 1436 cm^{-1} ($\nu_{COO\ bridging}$), and 912 cm^{-1} ($w_{CH2,\ vi}$) [33,17]. The two vinyl C=C stretching signals are attributed to the acid isomerization (H_3C–CH=CH–COOH and H_2C=CH–CH_2–COOH), and are also detected in commercial vinylacetic acid.

The solid state NMR spectrum of the solid clusters presents much more complicated spectral features than the liquid spectrum, since the main peaks have a higher multiplicity due to the non-averaged through-space interactions experienced by functional groups fixed in the crystalline structure. Thus, in order to define the cluster structures properly, we refer to the signals of ^{13}C and ^{1}H NMR spectra recorded on clusters dissolved in d_8-THF. We report here the signals of the functional groups involved in co-condensation and polymerization reactions, both in cluster formation and in hybrid system production. The assignment and the shifts in the peak position of the functional groups are detailed in relation to the precursor spectra [25]. Considering the spectral features of the pure liquid precursors –$Zr(OPr)_4$, VAA–, the precursor was presumably converted completely into ZrNBB. From ^{13}C NMR data (Table 1), it is clear that the formation of the Zr12 oxocluster leads to a small (+4 ppm) downfield shift of part of the terminal COOH signal at 178,4 ppm (C-4) as a result of its coordination to zirconium. The shift in position is also observed for the –CH_2– at 38,8 ppm (C-3, +4 ppm) and =CH– at 129,4 ppm (C-2, +1 ppm) of VAA and a small upfield shift is seen for =CH_2 at 119,1 (C-1, −1 ppm) [18,28,31–35]. This is consistent with the presence of terminal, chelating and bridging VAA functional groups determined by the ZrNBB crystalline structure. The vinylacetic acid can also isomerize in solution, forming the more stable 2-butenoic acid (see Scheme 1); this is clear from the proton spectrum of the dissolved cluster, although the related carbons signals (H_2C and CH) are not easy to detect.

The proton data (Table 2) confirm the previous conclusions, i.e. that the pristine zirconium alkoxide is completely hydrolyzed. The environment drives the VAA isomerization to the more stable 2-butenoic acid, identifiable from three new small peaks, the =CH signal at 6.75 ppm that correlates with the signals at 1.4 (CH_3) and 6.45 (=CH) ppm. The proton of the carboxyl group of VAA undergoes an upfield shift of −1.5 ppm in the cluster, resulting in an unresolved broad shoulder due to the different environments of the molecules. The shift refers to both VAA isomers, by comparison with the ^{13}C data.

Table 1
^{13}C NMR data of the ZrNBB dissolved in d8-THF and the pure precursors (signals labelled according to Scheme 1).

^{13}C Functional group	δ_{VAA}	$\delta_{Zr(OPr)4}$	δ_{ZrNBB}
4	178.4		182.0, 177.0
2	129.4		128.5 s
1	119.1		118.0 m
I		68 broad	
–CH_2–			43.0 m
3	38.8		
II		27.0	
III		10.0	

Table 2
^{1}H NMR data for the ZrNBB d8-THF and pure precursors. The numbering scheme refers to the proton attached to the numbered carbon, as shown in Scheme 1.

^{1}H Functional group	δ_{VAA}	$\delta_{Zr(OPr)4}$	δ_{ZrNBB}
4, 4a	11.6		10.1
2a, 2b	–		6.8, 6.5
2	5.6		–
3a, 3b	–		5.1
1	4.8		4.8
3	2.8		2.8
Aliphatic –CH_2–			1.4
I		3.8	
II		1.6	
III		0.9	

3.2. Characterization of thermal behaviour and polymerization process

The DSC study was undertaken to evaluate the thermal behavior of Zr oxoclusters and VTMS, the polymerization process of the pristine reagents and the effect of adding water on VTMS properties, with a view to gaining a better understanding the polymerization process of the hybrid O/I materials obtained and to optimizing the thermal curing process.

3.2.1. ZrNBB/BPO and VTMS/BPO systems

The DSC curve of ZrNBB was recorded up to 200 °C and presented two main endothermic peaks (Fig. 1a). The onset of the first endothermic effect, due to the loss of volatile species, occurred at a temperature around 110 °C. The principal effect, which appears broad and complex, is centered at 185 °C and is related to the partial decomposition of ZrNBB probably involving the release of carboxylate ligands. The whole mass loss is 19.1%, and increases to 27.5% if the analysis is performed up to 300 °C.

The process of thermal polymerization of ZrNBB, with BPO as initiator, is presented in Fig. 1b. The DSC curve of ZrNBB/BPO shows an exothermal peak centered at around 154 °C. The polymerization enthalpy of the vinyl groups of ZrNBB is about 240 J/g (926 kJ/mol). The sample recovered appears fragile after running the DSC up to 200 °C.

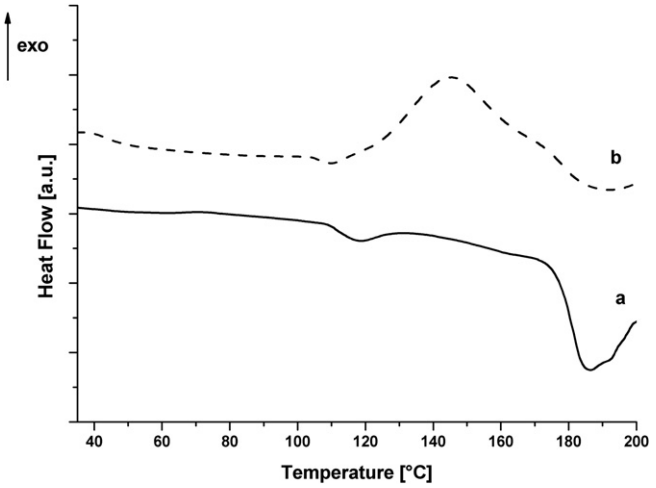

Fig. 1. DSC curves of ZrNBB (a) and ZrNBB/BPO (b).

The DSC curves of VTMS/BPO system, without and with VTMS pre-hydrolysis, are reported in Fig. 2. Pure VTMS polymerization cannot occur due to extensive evaporation [26,36–38] and the only event recorded in trace (a) of Fig. 2 is VTMS loss by evaporation, which accounts for the total weight loss.

On the other hand, the DSC curves of the pre-hydrolyzed VTMS/H_2O/BPO sol reacted for 2 and 18 h (Fig. 2b and c), show large endothermic peaks centred at 100 °C due to the release of the hydrolysis-condensation products (water and methanol). It was only after aging the sol for 48 h under stirring that a very weak exothermal polymerization peak due to the vinyl groups was detectable at 125 °C, along with the evaporation of hydrolysis-condensation by-products (Fig. 2d).

3.2.2. ZrNBB/VTMS/BPO hybrids

The polymerization reaction of ZrNBB/VTMS hybrid was studied in the sample prepared without any VTMS pre-hydrolysis step and compared with the DSC behavior observed for the sample prepared with VTMS pre-hydrolysis.

Fig. 3 shows the DSC curves recorded on the hybrid xerogels as a function of the Zr:Si molar ratio. The polymerization peak of Fig. 3a is produced by the overlapping of two events at about 120 and 150 °C, respectively, the former probably due to the VTMS vinyl groups and the latter to those of ZrNBB. In non-hydrolytic conditions, it is worth noting that the polymerization peak of VTMS is also observed in the sample with a low Zr oxoclusters load (Zr:Si = 1:20) (Fig. 3a). Increasing the ZrNBB load induces a change in the peak's shape together with a signal shift towards higher temperatures (Fig. 3, traces b–e). It is worth noting that using BPO calculated from both ZrNBB and VTMS avoids endothermal phenomena. In fact, we found that, if a smaller amount of BPO (0.5% wt of reagents) was used, the DSC curve of sample with Zr:Si molar ratio 1:1 showed two endothermic peaks at 120 and 180 °C respectively, which could be attributed to zirconium oxoclusters decomposition, giving rise to a slight increase in the opacity of the sample recovered after the DSC measurement. Table 3 shows the mass loss values measured during the first DSC scan. The sample with a Zr:Si molar ratio 1:20 shows the largest mass loss as a consequence of the relevant evaporation of VTMS. The weight loss is lower for the composition Zr:Si 1:10 and increases again for samples richer in ZrNBB.

For all samples, there were no residual polymerization peaks in the second DSC scan, and the recorded curves only presented T_g steps at temperatures depending on the amount of Zr oxocluster, These results are not shown here because the glass transition behavior is studied using dynamic mechanical thermal analysis and discussed later on.

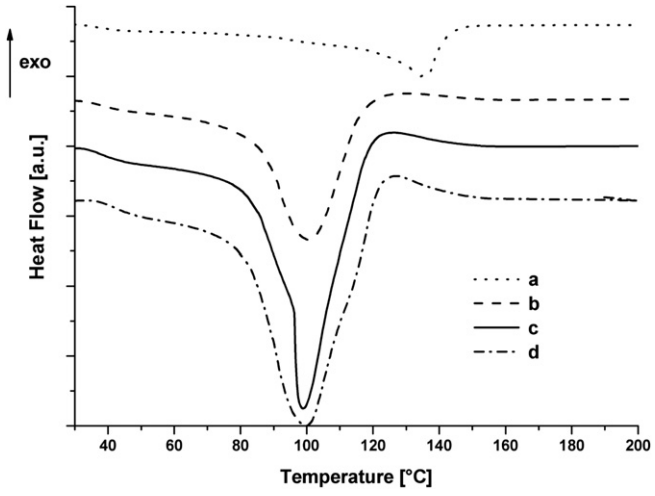

Fig. 2. DSC curves of VTMS/BPO (a), VTMS/H2O/BPO sol stirred for 2 h (b) 18 h (c) and 48 h (d).

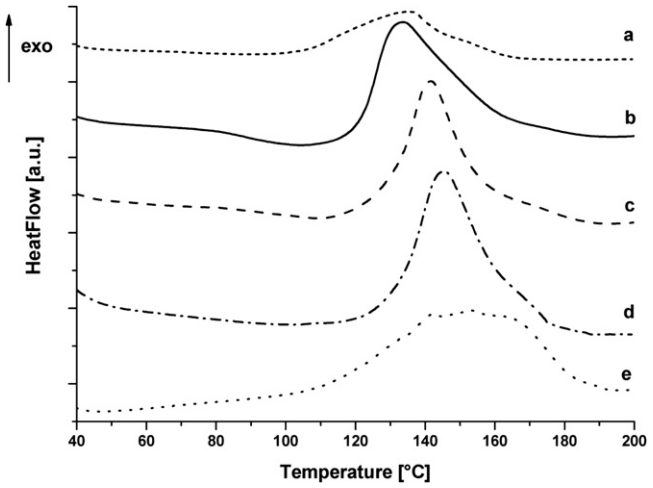

Fig. 3. DSC curves of ZrNBB/VTMS and BPO with molar ratio of 1:20 (a), 1:10 (b), 1:4 (c), 1:2 (d) and 1:1 (e).

The DSC study shows that polymerization is completed at high temperatures, but heating samples to 200 °C causes cracks in the polymeric specimens in the meantime. Two isothermal treatments were studied with a view to preventing cracks from forming during the polymerization and the preparation of bulk samples. Fig. 4 shows the DSC analyses of samples (Zr:Si 1:4) cured at 90 and 130 °C for 1 h. The comparison between the DSC traces shows that the polymerization is incomplete after curing at 90 °C (curve a) and a residual, small high temperature peak is observed after curing at 130 °C (curve b). The total polymerization heat measured for the sample cured at 90 °C is 112 J/g.

The hybrid samples prepared with VTMS pre-hydrolysis are colorless, whereas they are yellowish after non-hydrolytic synthesis. The DSC curves of these samples show endothermic phenomena in the range 110–140 °C and, immediately after, a small exothermal peak of polymerization. The release of volatile species during heating causes extensive cracking in the samples, so the hybrid polymers appear to be useless for high- or low-temperature applications. Table 4 gives the densities and soluble fraction (S) measured in water, n-hexane and toluene of the samples Zr:Si = 1:4, with and without the pre-hydrolysis step, measured on samples polymerized at 90 °C. With the pre-hydrolysis step, the samples are characterized by a lower density and higher soluble fraction, at least in H_2O and toluene at least. Polymerisation at 130 °C produces a general increase in density and reduction in S values.

Table 3
ZrNBB/VTMS hybrids without silane pre-hydrolysis: mass loss (Δm) measured during polymerization from DSC (0–200 °C), mass loss and T_g of polymeric specimens, recorded in the first DMS scan (0–300 °C).

Zr:Si molar ratio	1:1	1:2	1:4	1:10	1:20
$-\Delta m$ (%) (0–200 °C in DSC)	11.8	9.3	8.4	6.3	17.5
$-\Delta m$ (%) (0–300°C in DMS)	13.7	12.4	11.2	8.9	9.2
T_g (°C)	102 (±10 °C)	158 (±10 °C)	179 (±9 °C)	194 (±6 °C)	206 (±5 °C)

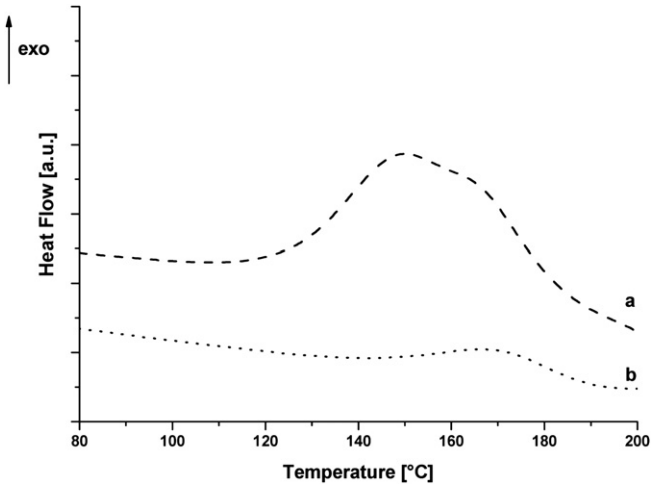

Fig. 4. DSC curves of ZrNBB/VTMS/BPO with Zr:Si molar ratio of 1:4 heat-treated at 90 °C (a) and 130 °C (b).

3.2.3. Thermo-mechanical measurements on ZrNBB/VTMS hybrids without silane pre-hydrolysis

It took several attempts to optimize the production of bulk ZrNBB/VTMS polymers suitable for studying their thermo-mechanical properties by dynamic mechanical spectroscopy (DMS). Based on above-mentioned DSC results for the sample with a molar ratio Zr:Si = 1:4, the xerogels were heated to 90 °C for 4 h, with a second curing step at 130 °C for 2 h. The density of the ZrNBB/VTMS (Zr:Si = 1:4) hybrid after treatment at 130 °C is 1.464 ± 0.005 and the specific surface area is low (below 2 $m^2\ g^{-1}$) with an average pore diameter of 40 Å.

The glass transition values given in Table 3 are very high, even if T_g is measured as the temperature corresponding to the maximum of G'' curve and not as the temperature of the maximum of tan δ [39]. If the VTMS content is increased, the T_g rises and the mass loss drops as a consequence of the greater degree of cross-linking of the hybrid network.

For all the samples, G' increases up to the T_g and then drops back in the first scan, whereas the initial G' value is much higher in the second scan, and no glass transition is visible. This accounts for an increase in the density of the polymer's network, which increases even more with increasing number of DMS scans.

Fig. 5a shows the G' values of the Zr:Si 1:4 sample measured at four different temperatures during each of 17 scans performed. It is worth noting that, as the number of scans increased, the G' values came closer and closer, overlapping in the last scans, and thereby indicating that a stable structural configuration had been reached, and that the organic polymerization and silica densification were complete. A loss of viscous behavior was accordingly recorded [40].

In the first DMS scan, the tan δ vs. temperature curve (Fig. 5b) shows several peaks, whereas the curves recorded in the subsequent scans are smoother and lower in intensity. Fig. 5c shows the tan δ values measured for the specimen Zr:Si 1:4 at different temperatures: it is worth noting that they fall to negligible values in the second scan. Table 5 shows the mass loss recorded during each DMS scan. The greatest loss was measured in the first scan and depended on the temperature range and heating rate.

The samples showed no cracks or other defects after multiple DMS scans, apart from the browning due to partial degradation of the organic moiety at 300 °C observed already after the first scan.

Table 4
Density and soluble fraction of ZrNBB/VTMS polymers (Zr:Si 1:4).

Samples	Density [g/cm^3]	S(H_2O)	S(*n*-Hexane)	S(Toluene)
ZrNBB/VTMS/BPO 90 °C	1.441 ± 0.005	7.6	10.6	13.4
ZrNBB/VTMS/BPO/H_2O 90 °C	1.395 ± 0.005	10.1	9.8	21.8

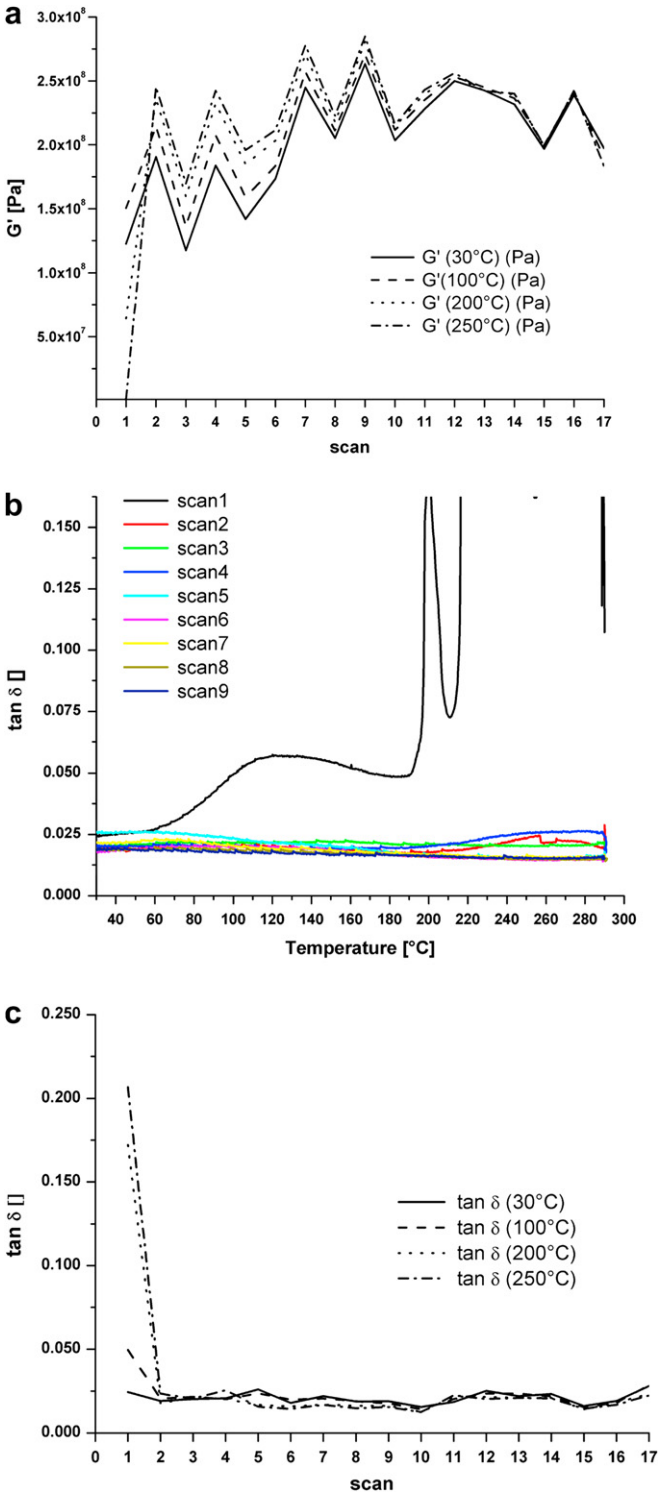

Fig. 5. Shear storage modulus measured (G') at 30, 100, 200 and 250 °C (a), tan d vs. temperature curves (b) and tan d measured at 30, 100, 200 and 250 °C (c) for each DMS scan of ZrNBB/VTMS/BPO sample having Zr:Si = 1:4.

Table 5
Mass losses drawn from DMS measurements on ZrNBB/VTMS (Zr/Si = 1:4) during17 subsequent scans (0–300 °C).

Scan	1	2	3	4	5	6	7	8	9	10	11	12	13	14	15	16	17
$-\Delta m$ (%)	11.2	0.0	0.8	0.2	0.2	0.3	0.0	0.0	0.1	0.0	0.0	0.1	0.3	0.1	0.1	0.0	0.0

3.3. Structural evolution vs. temperature of ZrNBB/VTMS hybrid without silane pre-hydrolysis

The structural evolution of the hybrid samples during the thermal treatment was studied by FTIR spectroscopy and the results recorded for the samples heated to 90 °C, 130 °C and the samples remaining after DSC analysis (after 1 scan up to 200 °C and after 5 following scans) were compared with the previously-reported spectrum of the ZrNBB/VTMS xerogel [25].

The main features of ZrNBB oxoclusters are recognizable in the spectrum of ZrNBB/VTMS xerogel [25] but the signals relating to carbonyl and the bridging acetate groups changes in position and intensity. It is worth noting the drop in intensity experienced by the C═O stretching at 1710 cm^{-1} due to the pristine carboxylic C═O. However, a new absorption vibration appears at 1769 cm^{-1}, in a position attributable to the C═O group of an ester. The signals due to the vinyl acetate groups occur at 3072 ($\nu_{as\ =CH2}$) and 3026 cm^{-1} ($\nu_{s\ =CH2}$), 1602 and 1644 cm^{-1} ($\nu_{C=C}$), 1544 and 1440 cm^{-1} ($\nu_{COO\ bridging}$), and 912 cm^{-1} ($w_{=CH2}$). The VTMS condensation process leads to the partial reduction in the intensity of the pristine Si–OCH_3 related vibrations (2843, 1194, 1090 and 774 cm^{-1}). A large band in the 1200–900 cm^{-1} region accounts for the Si–O–Si bonds and is generated by the overlapping of three main components (1124, 1036 and 1003 cm^{-1}), due to linear and cyclic oligosiloxanes. The vinyl group of VTMS can be detected from the typical signals at 3064 ($\nu_{as\ =CH2}$), 1598 ($\nu_{C=C}$), 1020 (δ_{CH}) and 974 cm^{-1} (w_{CH2}), which partially overlap the signals of the vinyl group of VAA.

The heat treatment at 90 °C (Fig. 6) leads to a marked reduction in the intensity of the C═O stretching vibration, which appears as a broad signal. The signals due to bridging acetate groups appear in the same position although their intensity has visibly decreased. The signals relating to the vinyl groups of VTMS (3064, 1598 cm^{-1}) are clearly detectable, while the vinyl groups of VAA have a lower intensity. The signal at 2843 cm^{-1} accounts for the presence of residual Si–OCH_3 groups at high temperatures, and there is still a shoulder after 5 repeated cycles up to 200 °C. Heating results in the broadening of the siloxane band due to the appearance of new components (Fig. 6). After 5 DSC scans, the siloxane band shows two main absorptions corresponding to the presence of cyclic structures at 1124 and 1036 cm^{-1} [41], the latter attributed to three Si units cycles. A new band appears at 437 cm^{-1}, related to the increase in short-range order of the siloxane network. After the DSC scans up to 200 °C, Si–OH absorption is clearly visible as a shoulder at 3650 cm^{-1}, attributed to hydrogen-bonded silanols [42].

The heat-treated hybrid samples were also characterized using multinuclear solid state NMR. Investigating different active nuclei, such as ^{29}Si, ^{13}C and ^{1}H gives the structural features of both inorganic and organic moieties.

Fig. 7 shows the ^{29}Si spectra recorded on samples after the same heat treatments as in the FTIR analysis. Thermal treatments of the ZrNBB/VTMS hybrid at 90 °C, 130 °C and 200 °C give rise to very similar spectra, with only T^2 {RSi$(OSi)_2$OR'} and T^3 {RSi$(OSi)_3$} units, located at −71.5 and −79.6 ppm, respectively with ratios of 46:54%, 39:59% and 51:43% indicating a partial consumption of the Si–OCH_3 functional groups [25].

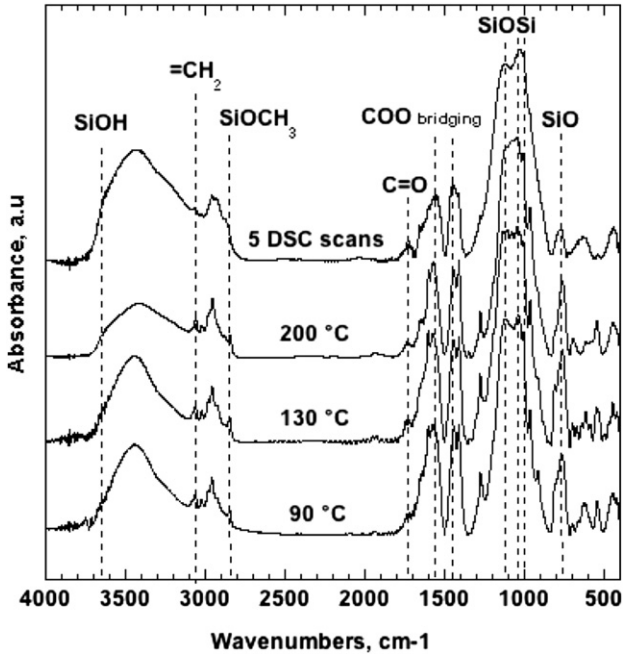

Fig. 6. FTIR spectra of ZrNBB/VTMS (Zr:Si = 1:4), treated at 90, 130, 200 °C and after 5 subsequent DSC scans.

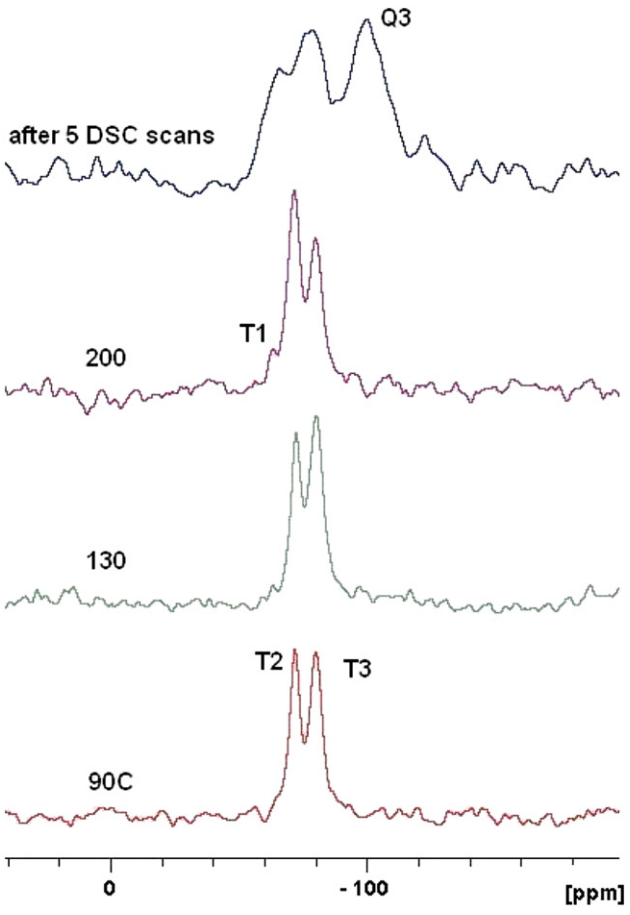

Fig. 7. ^{29}Si NMR spectra of the ZrNBB/VTMS (Zr:Si = 1:4) prepared without pre-hydrolysis and treated at different temperatures and after five DSC cycles.

There is an increase in T^2 intensity with respect to T^3 with increasing temperatures from 130 °C to 200 °C, without no shift in position. Derouet et al. [43] reported a similar behavior of VTMS grafted to silica beads. The samples treated at high temperature revealed a small T^1 peak at −62.9 ppm, accounting for 2% of the species observed at 130 °C and 6% at 200 °C. After 5 DSC scans (Fig. 7), there are still T^3 and T^2 units, but an increase of T^1 intensity and the presence of a new Q^3 broad peak at −99.8 ppm suggest a rearrangement of the siloxane network with both a greater degradation of the Si–OCH_3 group (confirmed by the small residual C-3′ peak) and partial breakdown of the Si–CH=CH_2 bond.

^{13}C NMR analysis is very important for following up the evolution of the organic counterpart in ZrNBB/VTMS hybrids (Fig. 8) [17]. At first, the polymerization step at 90 °C and subsequent curing at 130 °C do not seem to induce any major change in the organic moiety; in agreement with the results for ^{29}Si NMR, however, there are significant variations in the spectra of the sample after one and five DSC scan up to 200 °C.

In the heat-treated samples, new resonances at around 104.2 and 67 ppm and some other aliphatic CH_2 peaks in the region 20–40 ppm suggest an increase in the length of hydrocarbon chains of the original VAA and a partial esterification of the chain. These hypotheses are supported by the downfield shift and reduction in intensity of the main carbonyl resonance (C-4) and by the appearance of a new one (C-4a). [17] Moreover, the changes in intensity in the double bond region, between the peaks at 132.2 ppm (C-2) and 117.3 ppm (C-1), and the decrease in the residual C-3 peak at 39.3 ppm (which disappears altogether at 200 °C), combined with the increased methyl signal at 10 ppm (C-1a), demonstrate a progressive isomerization from vinylacetic acid to 2-butenoic acid. Although the isomerism already affects the oxocluster and its precursors, it increases with thermal treatment, resulting in a more difficult interpretation of the high temperature spectra.

The calculated areas of the signals confirm the above-described trends as a function of final treatment temperature. The relative integrals in the double bond region change; then, with respect to the C-2 peak, the new C-2a peak at 105 ppm increases with temperature from a third to half of the methine area at 118 ppm (C-2). This corresponds to a growth of the methyl peak at 10 ppm (C-1a).

The C-1 signal decreases together with an increase in the broad peaks in the 20–40 ppm region, accounting for the presence of aliphatic chains of different lengths.

After 5 subsequent DSC cycles, the ^{13}C NMR spectrum shows important changes in the structure of both the VAA and VTMS-derived portions (Fig. 8). A marked reduction in the intensity of the C-2, C-2a and C-3a double bonds and the disappearance of any C-1 resonance are accompanied by an increase in the intensity and broadening of the aliphatic region, due to double bond breaking. The C-3′ peak of the Si–OCH_3 group nonetheless remains.

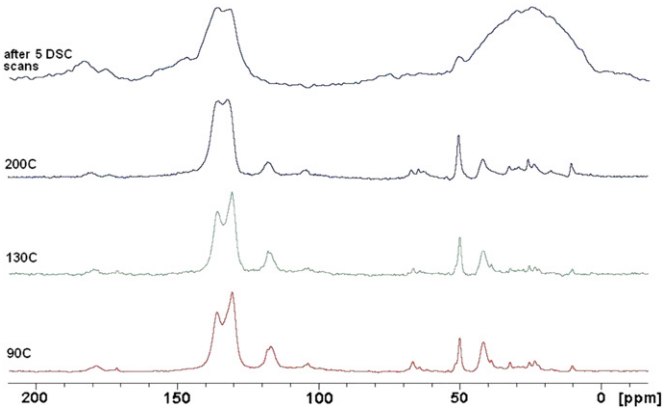

Fig. 8. ^{13}C NMR spectra of ZrNBB/VTMS prepared without pre-hydrolysis treated at different temperatures and after five DSC cycles up to 200 °C.

^{1}H NMR spectra of all the solid samples were recovered indirectly from 2D hetero-correlation experiments because of the large chemical shift anisotropy of proton peaks in the solid state. From Table 6, we can see that there is a partial hydrolysis of Si–OCH_3 with the formation of Si–OH bonds whose protons appear at 4.5 and 5 ppm in the 90 °C spectrum, and persists at 130 °C and 200 °C, according to the evolution of the T^1 and T^2 units in ^{29}Si spectra [44]. The new environment pushes the methoxy resonance downfield while the opposite happens to the vinyl protons. The broadening and general downfield shift of both the vinyl and the aliphatic CH_2 are indicative of a progressive increase in the hydrocarbon chain length due to VAA polymerization.

3.4. Structural characterization of ZrNBB/VTMS hybrid with silane pre-hydrolysis

For the sake of comparison the structural analysis was also performed on the pre-hydrolyzed samples and the results of ^{13}C and ^{29}Si NMR obtained for the Zr:Si = 1:4 sample treated at 130 °C are given in Fig. 9a and b, respectively.

There are two main features of note in the ^{13}C spectrum, i.e. the complete hydrolysis of the silane precursor (demonstrated by the absence of an OCH_3 peak at 50.6 ppm) and a greater tendency of the VAA to isomerize into 2-butenoic acid (demonstrated by the appearance of peaks at 172 and 18 ppm attributed to 4a and 1a, respectively). Integrating the corresponding two carbonyl signals gives us a ratio of VAA:2-butenoic acid of about 6:4. The relationship between the intensity of the peaks in the double bond region and the low intensity and broadness of the 2a and 3a resonances (around 125 and 145 ppm), together with the formation of alkyl chains in the 40–20 ppm region indicate some polymerization at the expense of both isomers.

The ^{29}Si NMR spectrum shows a good degree of condensation, revealed by the 51% of Si species involved in T^3 units (−79.0 ppm) and 34% in the T^2 units (−70.5 ppm). A broad signal in the −50 to −65 ppm range accounts for the residual 15%.

The FTIR analysis (Fig. 9c) also indicates a significant extent of condensation of the siloxane network. The siloxane band is generated by the overlapping of two peaks at 1136 and a 1034 cm^{-1}.

These signals can be attributed to the formation of cages with a large number of silicon units and open chain member siloxanes, respectively. The hydrolytic medium gives rise to a greater stability of the acid molecules linked to the Zr oxoclusters as shown by the

Table 6
^{1}H NMR data for the zirconium oxocluster and solid samples with a Zr:Si molar ratio of 1:4. The numbering scheme refers to the proton attached to the numbered carbon, as shown in Scheme 1.

Functional group	δ_{VTMS}	ZrNBB	ZrNBB/VTMS 90 °C	ZrNBB/VTMS 200 °C
4, 4a		10.1 broad	8.0 broad	8.0 broad
2a, 2b		6.8, 6.5	6.7 broad	6.9 broad
2′	5.8		6.1	5.9
1′	5.6		5.6	5.6
2		–	5.4	
3a, 3b		5.1	5.1	5.2
1		4.8		
Si–OH			4.5, 5.0	4.5
3′	3.2			
3		2.8	2.8–2.6	
Aliphatic –CH_2–		1.4		

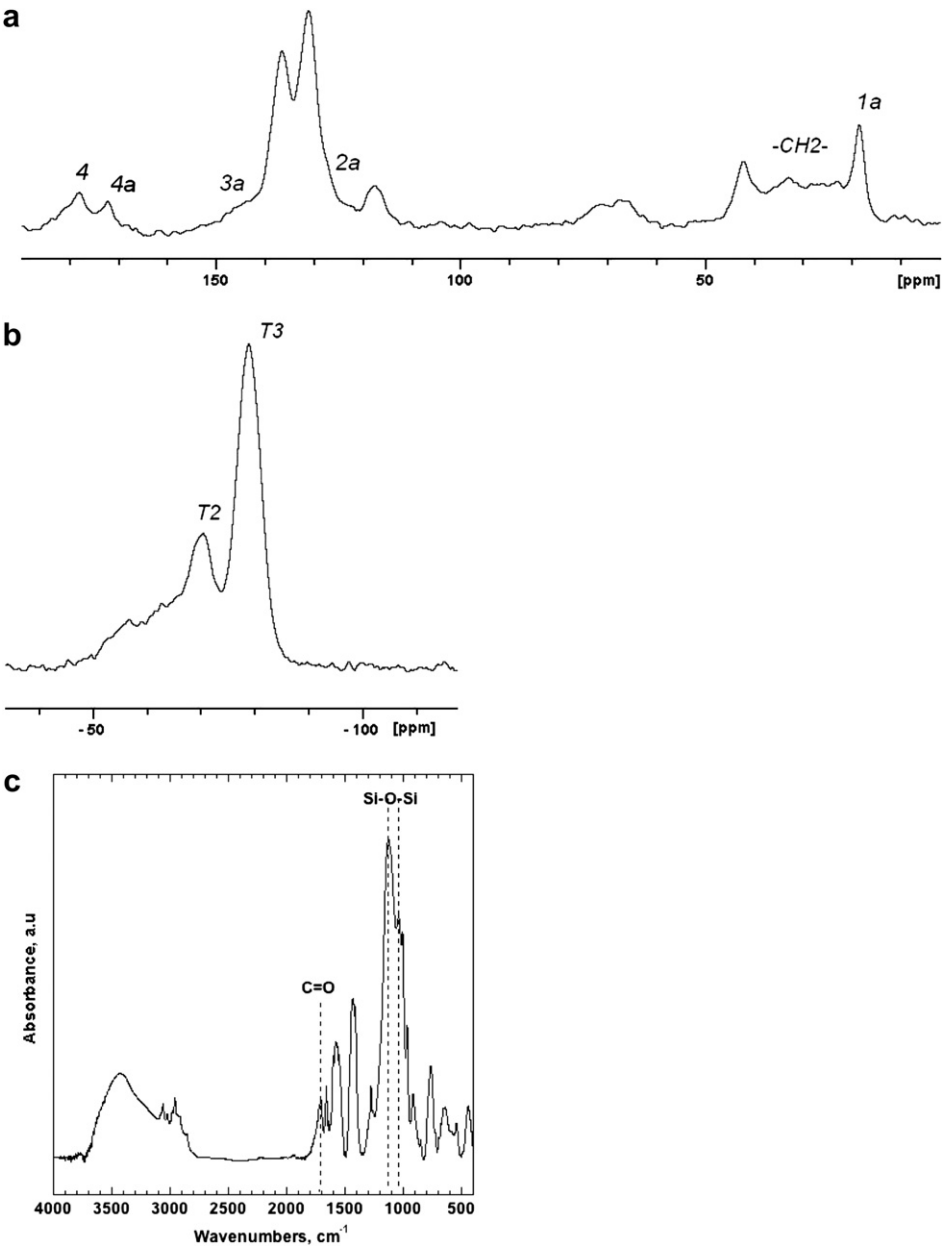

Fig. 9. (a) ^{13}C NMR; (b) ^{29}Si NMR, and (c) FTIR spectra of ZrNBB/VTMS (Zr:Si = 1:4), 130 °C with silane pre-hydrolysis.

greater intensity of the carbonyl bond signal (1710 cm^{-1}) by comparison with the signal found in the spectrum of the non-hydrolyzed sample (Fig. 6).

4. Discussion

This paper investigates the influence of the synthesis conditions on the preparation of hybrid O/I materials from ZrNBB and vinyl alkoxysilanes, particularly focusing on the influence on thermal and mechanical properties of preparing hybrids with or without vinyl alkoxysilane pre-hydrolysis step, i.e. working in a non-hydrolytic environment rather than in hydrolytic conditions.

Hybrid xerogels were obtained by reacting Zr12 clusters functionalized by vinyl acetate groups with VTMS in different molar ratio.

The structure of the Zr oxoclusters was assessed by FTIR and NMR studies and findings were consistent with data in the literature on similar Zr-based clusters. The thermal behavior of ZrNBB (Fig. 1b) after adding BPO indicates that the vinyl groups are able to polymerize over a wide temperature range (from 130 to 170 °C) as a consequence of the variable availability for radical polymerization of the VAA ligands, which have different arrangements in the ZrNBB structure. The material recovered at 200 °C, after the DSC scan, appears brittle.

The reaction between ZrNBB and VTMS without silane pre-hydrolysis step leads to the preparation of hybrid materials showing a valuable mechanical behavior, judging from DMS measurements. The study on the thermal polymerization of ZrNBB/VTMS/BPO samples indicates that even just a small amount of zirconium oxoclusters (Zr:Si = 1:20) can prevent VTMS loss by evaporation, and favors VTMS polymerization (Fig. 3a). The DSC study on pristine VTMS (Fig. 2) showed that VTMS evaporation is avoided if the organosilane is involved in the hydrolysis-condensation process by reaction with water. In the case of ZrNBB/VTMS

samples prepared without adding water, the hydrolysis-condensation of VTMS occurs due to the presence of the acid molecules hydrogen-bonded to the Zr oxocluster core, which can react with the methoxy groups for producing water *in situ* and the corresponding methyl ester. This interpretation is supported by the intensity decrease and the broadening of the signal due to the C=O stretching vibration, occurring at 1706 cm^{-1} in the FTIR spectrum of ZrNBB, after the reaction between oxocluster and VTMS.

Moreover, a partial condensation between the hydroxyl groups of zirconium oxoclusters and the methoxy groups of VTMS could also account for the lack of VTMS evaporation (Scheme 2). The polymerization peak of the sample with Zr:Si = 1:20 (Fig. 3a) results from the overlapping of at least two events at about 120 and 150 °C. If the ZrNBB content is increased (Fig. 3, traces b–d) the polymerization peak becomes sharper and shifts to higher temperatures. Since the DSC traces are not just the result of adding thermal effects belonging to the separated phases, the composition-dependent thermal evolution suggests the existence of chemical interactions between ZrNBB and the siloxane counterpart. With changing composition, the reaction between VTMS and zirconium oxoclusters might generate different species, from ZrNBB entrapped in the hybrid network (mainly) to oxoclusters involved in the formation of some hetero-metallic bonds (to a negligible extent), which probably have a different onset temperature and heat of polymerization.

The structural characterization does not provide clear evidence of the formation of hetero-metallic bonds at low temperatures. In the literature there are reports on questionable studies concerning the deconvolution of the T^2 signals and results with different Zr/Si ratios are compared in an attempt to prove the existence of the hetero-metallic bond [45,46]. In the ^{29}Si NMR spectrum, however, the shift between T^2 peaks related to Si–O–Zr and Si–O–Si bonds peaks is less than 2 ppm, making it hard to detect in solid state NMR, where peaks are definitely broad [47]. These studies are only valuable if they are supported by evidence from other analyses, mainly EXAFS or ^{17}O NMR, which require expensive ^{17}O-enriched samples [48,49].

The non-hydrolytic environment can favor the interaction between Si and Zr phases through oxo-bridges. In fact, it has been demonstrated that non-hydrolytic route enables a better control over the molecular-level homogeneity and stoichiometry of multicomponent oxides [41,50]. Indeed, the comparison with the results obtained on ZrNBB/VTMS/BPO samples prepared with a VTMS pre-hydrolysis step suggests a larger phase separation in the latter case. First of all, the gels are colorless, whereas they are yellowish in non-hydrolytic environment. Moreover, the DSC curves showed endothermic phenomena related to decomposition reactions beside the peak of exothermal polymerization peak. Under these experimental conditions, the reaction of the silane with water induces the growth of SiO_2-based domains (as indicated by the large amount of T_3 units in Fig. 9b) and also prevents the interaction with the ZrNBB clusters (Scheme 3). This is clearly confirmed by the intensity and sharpness of the signal due to the C=O stretching vibration in Fig. 9c. The pre-hydrolysis step allows extensive random silane condensation to occur before its condensation with zirconium oxoclusters.

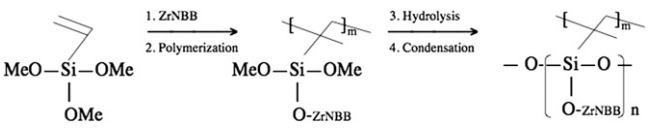

Scheme 2.

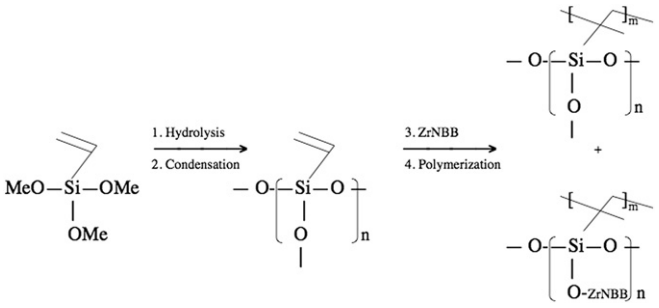

Scheme 3.

The formation of cyclic oligosilsesquioxanes thus appears to be facilitated, as shown by the FTIR spectrum (Fig. 9c) [50,51]. These oligomers can be released at higher temperature [27,48,52], leading to a greater mass loss than in the non-hydrolytic case and to extensive cracks in the samples. The limited interaction between ZrNBB and the siloxane counterpart leads to the decomposition of free zirconium oxoclusters, which are mainly entrapped into the siloxane network. From the solubility experiments, the soluble fraction measured on the pre-hydrolysed samples is higher than for the non-prehydrolysed samples, particularly in toluene, which dissolves the Zr oxoclusters. The soluble fraction drops with rising polymerization temperature as a consequence of the increased degree of cross-linking and density of the hybrid network.

On the other hand, the thermal behaviour of ZrNBB/VTMS samples prepared using the hydrolytic process makes these samples unfit for obtaining crack-free samples, whereas the thermal treatment at 90 and 130 °C of ZrNBB/VTMS samples produced in non-hydrolytic conditions enables the preparation of flawless bulk samples. Although the organic polymerization of the latter samples at 130 °C appears to be incomplete (Fig. 8), the specimens are suitable for DMS measurements.

It is worth of noting that, unlike the thermal behavior usually recorded for silica gel, the degree of siloxane condensation in the hybrid ZrNBB/VTMS material decreases with thermal curing (Fig. 7). The formation of new T^2 and T^1 units on heating up to 200 °C may be due to the rearrangement of the coordination sphere of the Zr oxoclusters linked to silicon through hetero-metallic bonds, indirectly confirming the previously-suggested chemical interaction between ZrNBB and VTMS. New Zr–O–Zr bridges could thus form at the expense of Zr–O–Si bridges due to the reaction with Zr–OH groups (Scheme 4). The silanol groups would be unable to react with other silanol groups, or with a cluster, unless they were sufficiently close. Moreover, the steric demand during the organic polymer formation might inhibit further siloxane condensation and even lead to stretching of the Si–O–Si bonds, with subsequent bond breaking. Indeed, Gunji et al. reported a drop in the degree of siloxane cross-linking with increasing degrees of polymerization in radically polymerized VTMS-derived gels [53].

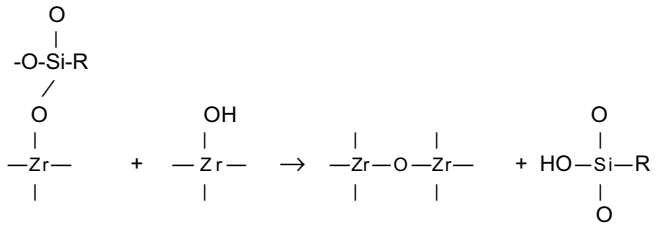

Scheme 4.

Running several thermal cycles leads to the occurrence of thermally-activated rearrangement reactions with the formation of *Q* units. The spectroscopic results collected on Zr:Si 1:4 sample after 5 DSC scans suggest an increase in both organic polymerization and phase separation, with the formation of segregated SiO_2–based domains (Fig. 7). The phenomenon is reasonable at these temperatures too, given the well-known behavior of the Zr heterometal ion, which acts as a catalyst for Si–C bond breaking already at 275 °C [52].

According to DMS results, the hybrid polymers show a thermosetting behavior. The T_g and mass loss values measured up to 300 °C (Table 3) depend on the silane content. Increasing the VTMS load leads to an increased degree of cross-linking of the hybrid network with no cracking or other defects, not even after several subsequent scans. The evolution of the shear storage modulus (Fig. 5a) indicates that the final structural configuration can be achieved through both organic and inorganic polymerization processes by increasing the number of subsequent scans.

5. Conclusions

This study deals with the reaction of VTMS, vinyl-acetate-substituted zirconium oxoclusters and BPO, with and without silane pre-hydrolysis, with a view to establishing which component and/or composition improves the interactions between organic polymer and inorganic metal oxides. The occurrence of organic polymerization and sol-gel process is the major issue if phase separation is to be avoided and homogeneity improved.

The formation of metal oxide networks via sol–gel process occurs typically in a hydrolytic environment, which leads to the random growth of large porous inorganic structures or phase separation, preventing a good radical polymerization. On the other hand, our results show that the non-hydrolytic environment promotes the organosilane condensation, producing very small silica-based domains, which could facilitate the radical polymerization of the organic part. The polycondensation of the metal oxide network, which takes place mainly by thermal cleavage at high temperature, is consequently less extensive and no longer induces thermal stress and fragility in the samples.

The absence of VTMS evaporation during the thermal polymerization is attributed to the hydrolysis-condensation reaction due to the carboxylic functions on the ZrNBB and to a partial condensation with the oxocluster suggested by their thermal behavior. FTIR and NMR analyses indicate the occurrence of organic polymerization in samples heated up to 130 °C. The hybrid polymers have high glass transition temperatures (above 100 °C), which increase with VTMS content. Samples retain shape and size due to the lack of viscous flow after glass transition. In fact, the glass transition disappears when the test is repeated. On repeating the thermal cycles, the rigidity increases and the rearrangement of the siloxane moiety is evident from the appearance of Q_3 units, which indicate an increased phase separation between the two components. The rearrangement is thermally activated and probably is facilitated by the oxocluster. The low polymerization is hardly surprising since this type of zirconium oxocluster has already been found to behave almost as an inhibitor during styrene polymerization [20]. However, even a partial interaction between the two networks is consistent with the thermosetting behaviour recorded during DMS analysis and provides extra benefits, such as making the hybrid polymers insoluble in solvents.

Acknowledgements

PRIN 2007 is acknowledged for partially funding this research.

References

[1] Miller JB, Ko EI. J Catal 1996;159:58–66.
[2] Soppera O, Croutxé-Barghorn C, Carre' C. Blanc D Appl Surf Sci 2002;186:91–8.
[3] Ivanovici S, Kickelbick G. J Sol-Gel Sci Technol 2008;46:273–80.
[4] Djourelov N, Suzuki T, Misheva M, Margac.a FMA, Miranda Salvado IM. J Non-Cryst Sol 2005;351:340–5.
[5] Wang H, Xu P, Zhong W, Shen L, Du Q. Polym Degrad Stabil 2005;87:319–27.
[6] Malenovska M, Litschauer M, Neouze MA, Schubert U, Peled A, Lellouche JP. J Organomet Chem 2009;694:1076–80.
[7] Malenovska M, Neouze MA, Schubert U. Dalton Trans 2008;34:4647–51.
[8] Brus J, Dybal J. Polymer 1999;40:6933–45.
[9] Saravanamuttu K, Min DX, Najafi SI, Andrews MP. Can J Chem 1998;76:1717–24.
[10] Park OK, Jung JI, Bae BS. J Mater Res 2001;16:2143–50.
[11] Oliveira DC, Macedo AG, Silva NJO, Molina C, Ferreira RAS, Andre PS, et al. Chem Mater 2008;20(11):3696–705.
[12] Armelao L, Gross S, Muller K, Pace G, Tondello E, Tsetsgee O, et al. Chem Mater 2006;18(25):6019–30.
[13] Armelao L, Eisenmenger-Sittner C, Groenewolt M, Gross S, Sada C, Schubert U, et al. Mater Chem 2005;15:1838–48.
[14] Armelao L, Bertagnolli H, Gross S, Krishnan V, Lavrencic-Stangar U, Müller K, et al. Mater Chem 2005;15:1954–65.
[15] Gross S, Zattin A, Di Noto V, Lavina S. Monatshefte Chem 2006;137(5):583–93.
[16] Puchegger S, Rennhofer H, Kogler FR, Loidl D, Bernstorff S, Schubert U, et al. Macromol Rapid Commun 2007;28:2145–50.
[17] Faccini F, Fric H, Schubert U, Wendel E, Tsetsgee O, Muller K, et al. Mater Chem 2007;17(31):3279–307.
[18] Puchberger M, Kogler FR, Jupa M, Gross S, Fric H, Kickelbick G, et al. Eur J Inorg Chem 2006;16:3283–93.
[19] Gao Y, Kogler FR, Schubert U. J Polym Sci Part A Polym Chem 2005;43:6586–91.
[20] Kogler FR, Koch T, Peterlink H, Seidler S, Schubert U. J Pol Sci Part B Pol Phys 2007;45:2215–31.
[21] Kogler FR, Schubert U. Polymer 2007;48:4990–5.
[22] Sangermano M, Gross S, Pacella L, Priola A, Rizza G. Macromol Chem Phys 2007;208(16):1730–6.
[23] Basch S, Gross S, Choudhury NR, Matisons JJ. Sol-Gel Sci Technol 2005;33:39–45.
[24] Rosez L, Fornasieri G, Trabelsi C, Creton C, Zafeiropoulos NE, Stamm M, et al. Prog Solid State Chem 2005;33:127–35.
[25] Di Maggio R, Dirè S, Callone E, Girardi F, Kickelbick GJ. Sol-Gel Sci Technol 2008;48:168–71.
[26] Chen LF, Cai ZH, Zhou W, Lan L, Chen XJ. J Mat Sci 2005;40:3497–501.
[27] Dirè SJ. Sol-Gel Sci Technol 2003;26:28–34.
[28] Piszczek P, Radtke A, Wojtczak A, Muziol T, Chojnacki J. Polyhedron 2009;28:279–85.
[29] Piszczek P, Radtke A, Wojtczak A, Grodzicki A, Chojnacki J. Polyhedron 2007;26:679–85.
[30] Girardi F, Graziola F, Aldighieri P, Fedrizzi L, Gross S, Di Maggio R. Prog Org Coat 2008;62:376–81.
[31] Kogler FR, Jupa M, Puchberger M, Schubert UJ. Mat Chem 2004;14:3133–8.
[32] Schubert UJ. Sol-Gel Sci Technol 2003;26:47–55.
[33] Sangermano M, Gross S, Priola A, Rizza G, Sada C. Macromol Chem Phys 2007;208(23):2560–8.
[34] Yoshikawa M, Motoi T, Tsubouchi KJ. Macromol Sci Part A 1999;36(4):621–31.
[35] Brar AS, Singh G, Shankar R. Polymer 2005;46:7164–75.
[36] Kang JW, Kim BR, Kang GG, Moon MS, Choi BG, Ko MJ. Mat Res Soc Symp Proc 2004;812:1–6.
[37] Jiao C, Wang Z, Gui Z, Hu Y. Eur Polym J 2005;41:1204–11.
[38] Seno M, Hasegawa M, Hirano T, Sato TJ. Pol Sci A Pol Chem 2005;43(23):5864–71.
[39] Rieger J. Polym Test 2001;20:199–204.
[40] Mammeri F, Le Bourhis E, Rozes L, Sanchez C. J Mat Chem 2005;15:3787–811.
[41] Dirè S, Tagliazucca V, Brusatin G, Bottazzo J, Fortunati I, Signorini R, et al. J Sol-Gel Sci.Technol 2008;48:217–23.
[42] Innocenzi P. J Non-Cryst Solids 2003;316:309–19.
[43] Derouet D, Foregard S, Brosse JC, Emery JL, Buzare JY. J Pol Sci A Pol Chem 1998;36:437–53.
[44] Brus J, Dybal J. Polymer 2000;41:5269–82.
[45] Degirmenci V, Erdem OF, Ergun O, Yilmaz A, Michel D, Uner D. Top Catal 2008;49:204–8.
[46] Pickup DM, Mountjoy G, Wallridge GW, Newport RJ, Smith ME. Phys Chem 1999;1:2527–33.
[47] Ivanova Y, Geranova TS, Dimitriev Y, Miranda Salvado IM, Fernandes MHV. Thin Solid Films 2006;515:271–8.
[48] Hoebbel D, Reinert T, Schmidt H. J.Sol-Gel Sci Technol 1996;6:139–49.
[49] Vioux A., Chem. Mater. 1997; 9: 2292–2299
[50] Di Maggio R, Fambri, Cesconi M, Vaona W. Macromolecules 2002;35:5342–6.
[51] Orel B, Jese R, Vilcnik A, Lavrencic Stangar U. J Sol-Gel Sci Technol 2005;34:251–65.
[52] Dirè S, Campostrini R, Ceccato R. Chem Mater 1998;10:268–73.
[53] Gunji T, Kawaguchi Y, Okonogi H, Sakan T, Arimitsu K, Abe Y. J Sol–Gel Sci Technol 2005;33:9–13.